Micromagnetics of ultrathin films with perpendicular magnetic anisotropy

R. Skomski,* H.-P. Oepen, and J. Kirschner
Max-Planck-Institut für Mikrostrukturphysik, Weinberg 2, 06120 Halle, Germany
(Received 6 March 1998)

Magnetization processes in ultrathin transition-metal films with perpendicular magnetic anisotropy are investigated. By model calculations it is shown that nucleation in ideal films is incoherent and therefore bulklike, whereas the truly ultrathin limit of coherent nucleation is restricted to film patches of small cross-section areas. In ideal monolayers, the nonzero film thickness leads to bulklike nucleation if the lateral dimensions of the film exceed about 1 μm. This means that monolayer patches having submicrometer diameters cannot be regarded as ultrathin in a micromagnetic sense. On the other hand, the critical single-domain diameter of ultrathin films is larger by one order of magnitude than expected from bulk-type thin-film calculations.
[S0163-1829(98)07429-3]

I. INTRODUCTION

Traditionally, ultrathin magnetic films are defined in terms of absolute thickness, measured, for example, in monolayers, or relative values such as the thickness of a film patch divided by its lateral dimensions. Although this approach is reasonable from the point of view of electronic structure and geometry, it neglects the long-range nature of magnetostatic dipole interactions epitomized by the magnetostatic self-interaction energy $E_{\rm MS}=-(\mu_0/2)\int \mathbf{M}\cdot\mathbf{H}'\,d\mathbf{r}$, where

$$\mathbf{H}'(\mathbf{r}) = \frac{1}{4\pi}\int \frac{3(\mathbf{r}-\mathbf{r}')(\mathbf{r}-\mathbf{r}')\cdot\mathbf{M}(\mathbf{r}')-(\mathbf{r}-\mathbf{r}')^2\mathbf{M}(\mathbf{r}')}{(\mathbf{r}-\mathbf{r}')^5}\,d\mathbf{r}'. \tag{1}$$

This refers in particular to films with perpendicular magnetic anisotropy,[1–9] whereas the main effect of magnetostatic interactions in films with easy-plane anisotropy is to confine the magnetization to the film plane.[10,11] To illustrate the difference, we approximate the thin film by a homogeneously magnetized ellipsoid of revolution of volume V whose radius $R_x=R_y=R$ is much larger than the ''film thickness'' $2R_z$. The magnetostatic self-interaction energy is then given by $D\mu_0M^2V/2$, where $D\approx 1$ and $D\approx 0$ are the demagnetizing factors for in-plane and perpendicular magnetization orientations, respectively (see, e.g., Ref. 11). The energy fractions stored inside and outside the magnet are D and $1-D$, respectively, so that the magnetostatic self-interaction energy of thin films with perpendicular anisotropy is stored *inside* the films.[12]

An important point is that incoherent (nonuniform) magnetization configurations such as domains reduce the magnetostatic energy of thin films with perpendicular anisotropy. However, the reduction of the magnetostatic energy on domain formation is not very strong, because the demagnetizing factors of the film patches remain close to $D\approx 1$ and the magnetostatic interactions between the domains are small. Furthermore, the reduction has to compete against exchange and anisotropy contributions, and in practice external magnetic fields may be necessary to realize deviations from the uniform magnetization.

In the past, thin films with perpendicular anisotropy were made from noncubic bulk materials such as MnBi and $BaFe_{12}O_{19}$.[4–6] However, the thickness t of those films, typically of order 100 nm, greatly exceeds micromagnetic lengths such as the domain-wall width, which is at most of order 10 nm for the films considered. A fairly recent development is the deposition and investigation of *ultrathin* transition-metal films with perpendicular anisotropy.[1,7,9] It is now possible to produce nearly ideal ultrathin film patches having diameters of order 50 nm and containing more than 10 000 atoms (see, e.g., Ref. 13).

In this paper we deal with the effect of long-range magnetostatic interactions on the magnetic behavior of ultrathin films. In particular, we investigate whether the nucleation of magnetic reversal is coherent[11,14–16] (Fig. 1) and whether the energetically most favorable spin configuration is free of reverse magnetic domains separated by Bloch walls[4,17–21] (Fig. 2).

II. NUCLEATION

Nucleation occurs when an external magnetic field $\mathbf{H}=-H_N\mathbf{e}_z$ destabilizes the remanent magnetization state $\mathbf{M}=M_s\mathbf{e}_z$. In the case of very small spherical particles, the Zeeman and anisotropy energies $-\mu_0M_zH_zV$ and $-K_1VM_z^2/M_s^2$, respectively, yield the well-known nucleation field $2K_1/\mu_0M_s$, where K_1 is the first uniaxial anisotropy constant.[14,15] In general, however, one has to include the interatomic exchange-energy density $A[\nabla\cdot\mathbf{M}(\mathbf{r})]^2$, where A is the exchange stiffness, and the local magnetostatic interaction field, Eq. (1).[14,15] Since the local magnetization $\mathbf{M}(\mathbf{r})$ is largest near the atomic nuclei, the integral Eq. (1) can be approximated by a sum over atomic moments $\boldsymbol{\mu}_i=\int_{\rm at}\mathbf{M}(\mathbf{r}-\mathbf{R}_i)d\mathbf{r}$ at positions $\mathbf{R}_i$. Careful analysis of Eq. (1), similar to that on p. 187 in Ref. 11, yields two contributions quadratic in the small quantity $\mathbf{m}(\mathbf{r})=\mathbf{M}(\mathbf{r})-M_s\mathbf{e}_z$. First, putting $\mathbf{M}=M_s\mathbf{e}_z$ in Eq. (1) yields a local field that can be interpreted as a trivial addition to the external field $\mathbf{H}$. Second, there is a magnetostatic self-interaction between de-

 © 1998 The American Physical Society

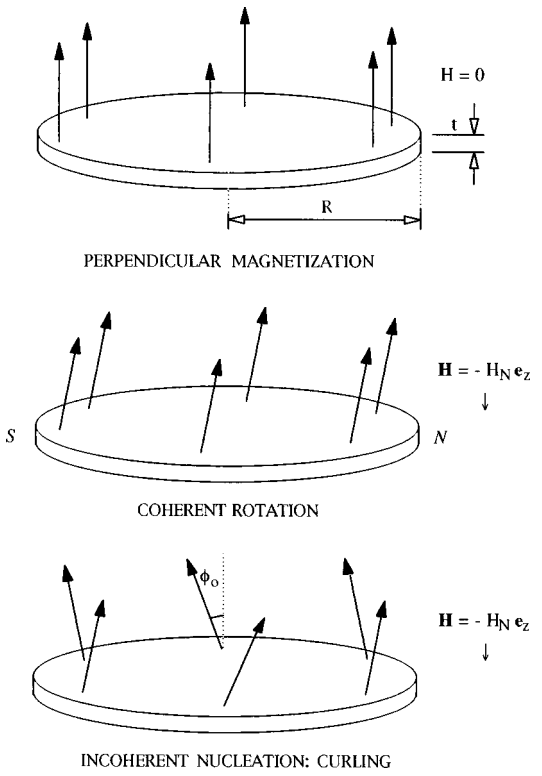

FIG. 1. The onset of magnetic reversal (nucleation).

viations $\mathbf{m}(\mathbf{r})$ and $\mathbf{m}(\mathbf{r}')$. On a macroscopic scale, this self-interaction outweighs the exchange interaction and gives rise to incoherent nucleation modes such as curling.[11,14,15] The point, illustrated in Fig. 1, is that coherent rotation exhibits a magnetization component in the x-y plane that leads to magnetostatically unfavorable poles at the film edges. By contrast, magnetization curling costs some exchange energy but is magnetostatically favorable. Because exchange interaction ensures parallel spin alignment on an atomic scale, there is a critical radius R_{coh} above which nucleation is curlinglike and below which it is coherent.

A. Scaling analysis

Let us start with the determination of R_{coh} from scaling arguments. On the one hand, incoherent nucleation costs exchange energy of order $-J\cos\phi$ per pair of neighboring atoms, where ϕ denotes the angle between the atomic moments and J is the interatomic exchange constant. Adding the exchange contributions of all pairs of neighbors we find a total exchange-energy contribution of order $Jt\phi_0^2/a$, where t is the film thickness, a is the interatomic distance, and ϕ_0 is an angle describing the maximum local deviation from the perpendicular magnetization state (Fig. 1). Note that the exchange stiffness A scales as J/a.[15] On the other hand, from the magnetostatic self-energy, which can be rewritten as

$$E_{\mathrm{MS}}=\frac{\mu_0}{8\pi}\int\frac{\nabla\cdot\mathbf{M}(\mathbf{r})\nabla\cdot\mathbf{M}(\mathbf{r}')}{|\mathbf{r}-\mathbf{r}'|}\,d\mathbf{r}\,d\mathbf{r}', \tag{2}$$

we deduce that the gain in magnetostatic energy is proportional to $\mu_0 M_s^2 t^2 R\phi_0^2$. By equating the magnitudes of the competing energies we obtain the coherence length

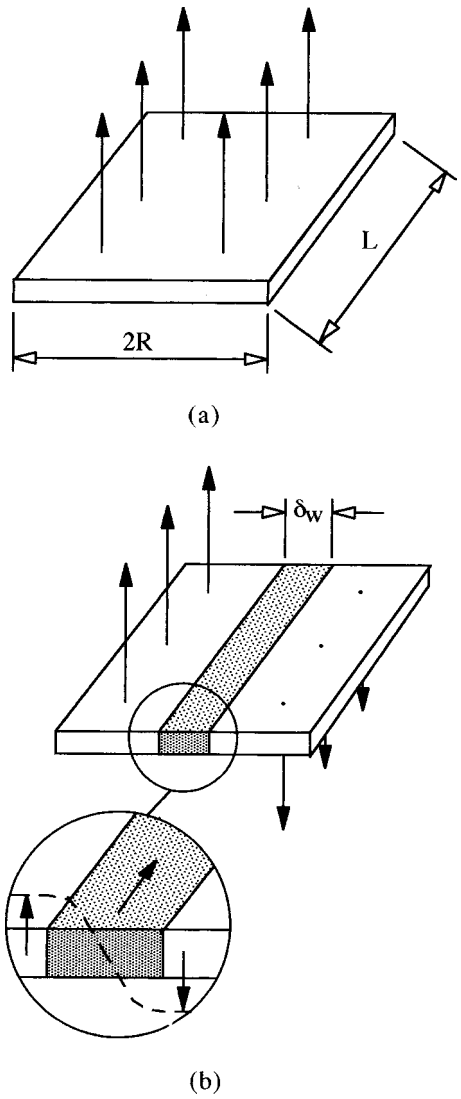

FIG. 2. Domain formation in ultrathin films with perpendicular magnetic anisotropy: (a) single-domain state and (b) two-domain state.

$$R_{\mathrm{coh}}=c\,\frac{J}{\mu_0 M_s^2 ta}, \tag{3}$$

where c is a geometry-dependent dimensionless prefactor.

The important result, Eq. (3), means that nucleation is curlinglike if the cross-section area of the film, scaling as Rt, exceeds some critical area of order $J/a\mu_0 M_s^2$. By contrast, it is not possible to define a thickness or a ratio t/R below which nucleation reaches the ultrathin limit of being coherent rather than curlinglike.

To discuss the critical area in terms of relativistic quantum mechanics we exploit that condensed-matter interatomic distances, magnetizations, and exchange energies scale as a_0, μ_B/a_0^3, and $e^2/(4\pi\varepsilon_0 a_0)$, respectively. With Bohr's hydrogen radius $a_0=4\pi\varepsilon_0\hbar^2/me^2=0.5292$ Å and Sommerfeld's fine-structure constant $\alpha=e^2/4\pi\varepsilon_0\hbar c\approx\frac{1}{137}$ we obtain the fundamental magnetic length $l_0=a_0/\alpha=7.252$ nm, whose square gives the order of magnitude of the critical area. In a sense, l_0 is a fundamental magnetic interaction length as μ_B is a fundamental atomic moment. However, the

magnetic moments $0.6\mu_B$, $1.7\mu_B$, and $2.2\mu_B$ for Fe, Co, and Ni, respectively, illustrate that μ_B and l_0^2 yield orders of magnitude rather than exact values.

B. Numerical aspects

The prefactor c in Eq. (3) is difficult to calculate because there is no general solution of the nucleation problem. To estimate c we model the film as a continuous oblate ellipsoid of revolution whose aspect ratio $R_z/R_x = t/2R$ is small. Comparing the known nucleation fields for coherent rotation and curling[11,14,15] we obtain

$$R_{\mathrm{coh}} = \frac{2q(D)}{\sqrt{1-D}}\, l_{\mathrm{ex}}. \tag{4}$$

Here $D = D_z$ is the demagnetizing factor of the ellipsoid, q is the root of an equation involving spheroidal Bessel functions,[11] and $l_{\mathrm{ex}} = \sqrt{A/\mu_0 M_s^2}$ is the magnetostatic exchange length. Note that demagnetizing fields $-DM_z$ are defined for homogeneous ellipsoids only[11] and must not be confused with the more general phenomenon of local magnetic fields[1] in nonellipsoidal and inhomogeneous films. Since A is of order J/a, the exchange length l_{ex} is proportional to l_0. Typical orders of magnitude are $A = 10^{-11}$ J/m and $\mu_0 M_s = 1$ T, respectively, so that $l_{\mathrm{ex}} \approx 3$ nm for a wide range of thin films and bulk materials.[22]

As found by Aharoni, q varies smoothly as a function of the aspect ratio and approaches the value 2.115 in the thin-film limit.[11,16] Up to a weakly shape-dependent prefactor, the coherence length of bulk materials is therefore of order l_0. In the ''truly ultrathin'' limit of vanishing film thickness, the demagnetizing factor approaches $D = 1$, so that R_{coh} goes to *infinity*. In real films, where the aspect ratio t/R is small but nonzero, $D = 1 - \pi t/4R$,[23] and we obtain after short calculation

$$R_{\mathrm{coh}} = 22.78\, \frac{A}{\mu_0 M_s^2 t}. \tag{5}$$

Using bulk values[22] of A and M_s and taking $t = 2$ Å yields the coherence radii 256 nm, 456 nm, and 1240 nm for Fe, Co, and Ni, respectively. Nucleation in fictitious ideal monolayers having lateral areas much larger than about 1 μm^2 is therefore curlinglike, whereas coherent nucleation is expected in patches up to a few hundred nm in diameter. In turn, fictitious films having a diameter of 1 mm have to be as thin as about 0.003 Å to reach the ultrathin limit of nucleation.

At this point it is worthwhile emphasizing that the nonellipsoidal shape of real thin films does not only modify the constant c but also introduces a minor degree of incoherence in the (essentially) coherent mode. A more subtle problem is local inhomogenities such as atomic defects. The formal analogy between quantum mechanics and micromagnetics[24] means that the influence of morphological disorder on nucleation is equivalent to the Anderson localization of one-electron wave functions.[25] In truly infinite films ($R = \infty$), this causes the nucleation modes $\mathbf{m}(\mathbf{r})$ to localize even if the disorder is arbitrarily weak. This incoherent localization dominates in real monolayer films of macroscopic lateral dimensions,[8,26] whose magnetic description goes beyond the scope of this work. Note, finally, that the nucleation-field difference $\pi t M_s/8R$ associated with the transition from coherent to incoherent nucleation is at most of order mT, so that the implications of Eqs. (3) and (5) pose a challenge to experimental verification.

III. DOMAIN FORMATION

The nucleation problem, which refers to the stability of an aligned magnetization configuration, is only one aspect of ultrathin-film micromagnetics. Another aspect is the existence and size of equilibrium domains in the remanent state ($H = 0$). The size of magnetic domains in infinite ultrathin films with perpendicular anisotropy has been investigated in a number of works.[4,17–21] Málek and Kambersk\'y[4] considered domains in MnBi films, where perpendicular anisotropy is associated with the hexagonal NiAs structure of the bulk material. That approach, which has been extrapolated to ultrathin films by Kaplan and Gehring[19] and Millev,[20] neglects the domain-wall width δ_w. Domain walls in MnBi films are indeed narrow compared to the film thickness, but in ultrathin films $\delta_w \gg t$.

Here we will focus on the existence of domains in ultrathin films with perpendicular anisotropy rather than calculating domain sizes. In general, domains are energetically favorable if the size of the magnet exceeds some critical value. For example, in hard-magnetic bulk particles the critical single-domain radius $R_{\mathrm{SD}} \approx 36\pi l_{\mathrm{ex}}^2/\delta_w$ reflects the competion between the wall energy, scaling as $R^2\sqrt{AK_1}$, and the gain in magnetostatic energy on domain formation, which is of order $R^3\mu_0 M_s^2$.[27] To investigate the thin-film limit of domain formation we consider a stripe of thickness t, width $2R$, and length $L \gg R$, and calculate the half-width R_0 above which the formation of two parallel domains is energetically favorable (Fig. 2).[28] Since the relevant micromagnetic lengths, namely, $l_{\mathrm{ex}} \approx 3$ nm and $\delta_w \approx \pi\sqrt{A/K_1} \approx 5$ nm, are much larger than the interatomic spacing, we can start from the continuous energy functional

$$E_M = \int \left[A\, \frac{(\nabla \mathbf{M})^2}{M_s^2} - K_1\, \frac{(\mathbf{M}\cdot\mathbf{e}_z)^2}{M_s^2} - \mu_0 \mathbf{M}\cdot\mathbf{H} - \frac{\mu_0}{2}\, \mathbf{M}\cdot\mathbf{H}' \right] d\mathbf{r}. \tag{6}$$

Due to the high surface anisotropy K_s, K_1 equals $2K_s/t$. By putting $\mathbf{M}(\mathbf{r}) = M_s \cos\phi(x)\mathbf{e}_z + M_s \sin\phi(x)\mathbf{e}_y$ inside the film we obtain the magnetostatic energy

$$E_{\mathrm{MS}} = \frac{\mu_0 M_s^2}{2}\, Lt \int s^2(x)\, dx + \frac{\mu_0 M_s^2}{8\pi}\, Lt^2 \int s'(x) s'(x') \ln \frac{|x-x'|}{t}\, dx\, dx' \tag{7}$$

as a function of the z component $s(x) = M_z(x)/M_s$ of the magnetization.[29] Minimizing the total energy, Eq. (6), with respect to $s(x)$ yields the magnetization profile of the two-domain state, including that of the wall. Note that the first

term on the right-hand side of Eq. (7) and the anisotropy energy $-K_1 L t \int s^2(x)dx$ have the same structure, so that the anisotropy enters the theory in the form of the renormalized constant $K = K_1 - \mu_0 M_s^2/2$. This gives a theoretical justification of the use of effective anisotropy constants[2] to discuss experimental data.

Using the self-consistent Bloch-wall ansatz $s(x) = -\tanh(x/\delta)$ and Eq. (7), we obtain the energy change on domain formation

$$\frac{\Delta E}{Lt} = 2K\delta + \frac{2A}{\delta} + \frac{\mu_0 M_s^2 t}{\pi} \ln \frac{c_w \delta}{R}. \tag{8}$$

Here the numerical coefficient $c_w \approx 1.356$ reflects the internal structure of the Bloch wall. Minimizing Eq. (8) with respect to δ yields, up to a negligibly small thickness-dependent contribution, $\delta = \sqrt{A/K}$ and $\delta_w = \pi\sqrt{A/K}$. The sought-for width R_0 is obtained by putting $\Delta E = 0$ in Eq. (8),

$$R_0 = c_w \delta \exp\left(\frac{\pi\gamma}{\mu_0 M_s^2 t}\right), \tag{9}$$

where $\gamma = 4\sqrt{AK}$ is the wall energy.

The quantity R_0 is closely related to the domain width W of stripe-domain patterns. Comparing Eq. (9) with[20]

$$W = \frac{\pi t}{2\sqrt{e}} \exp\left(\frac{\pi\gamma}{\mu_0 M_s^2 t}\right), \tag{10}$$

we see that the main difference is a prefactor of order $\delta/t \approx 10$, whereas the leading exponential term remains unchanged. In other words, the presence of walls much wider than the film thickness leads to a pronounced magnetostatic decoupling of neighboring domains, and the trend towards domain formation is even smaller than predicted by the Kaplan-Gehring-Millev theory.

IV. DISCUSSION AND CONCLUSIONS

It is interesting to note that the factor δ/t by which Eq. (10) differs from Eq. (9) does not reflect the presence or absence of long-wavelength periodicity but is a ''short-wavelength'' effect associated with the nonzero domain-wall width. A physical interpretation is that the magnetostatic field acting on the spins in the middle of the wall is zero by symmetry. This means that the wall center does not yield magnetostatic contributions going beyond the local demagnetizing term $\mu_0 M_s^2/2$. From a magnetostatic point of view, this is equivalent to the removal of a slice or stripe of thickness $\Delta \approx \delta_w$ containing the central part of the wall. The missing slice reduces the field H' acting on neighboring domains and weakens the trend towards domain formation. By considering a half-plane with perpendicular magnetization and $t \ll \Delta$ we obtain the bounds $\mathbf{H}' = \pm M_s t/2\pi\Delta$. By contrast, for $t \gg \Delta$ the removal of the slice is a small perturbation and $\mathbf{H}'$ remains of order M_s.

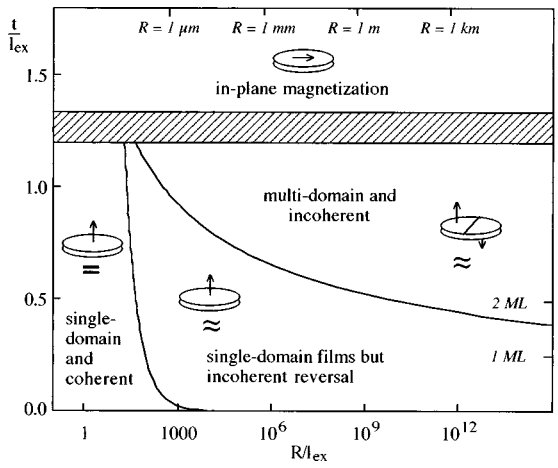

FIG. 3. Magnetic phase diagram for ultrathin films with perpendicular anisotropy, $l_{ex} = 2$ nm, and $K_s = 0.5$ mJ/m^2. The dashed area denotes intermediate thicknesses where higher-order anisotropy constants are important.

On the other hand, it can be shown that Eq. (9) is compatible with the numerical square-lattice calculations by Yafet and Gyorgy,[17] where no analysis of the ultrathin limit was performed. The proof is straightforward but somewhat cumbersome because it involves a number of parameter substitutions and series expansions going beyond the scope of this paper.

The nucleation and domain-formation behavior of the films is summarized in the schematic phase diagram (Fig. 3). The transition from perpendicular to in-plane configurations has been discussed elsewhere (see, e.g., Ref. 17) and is of minor interest in the present context. In the ultrathin limit, the film patches are single domain, and well-defined films such as monolayers exhibit a transition from coherent to incoherent nucleation at R_{coh}. This transition is also encountered in hard-magnetic single-domain bulk particles,[22] where $R_{SD} \gg l_{ex}$, but does not occur for $t/l_{ex} = 0$. In this sense, monolayer films behave as bulklike rather than reaching a truly ultrathin limit.

*Author to whom correspondence should be addressed. Present address: Behlen Laboratory, University of Nebraska Lincoln, Lincoln, NE 68588-0113.

Electronic address: rskomski@unlinfo.unl.edu

[1] B. Heinrich, J. F. Cochran, M. Kowalewski, J. Kirschner, Z. Celinski, A. S. Arrott, and K. Myrtle, Phys. Rev. B **44**, 9348 (1991).

[2] M. Speckmann, H. P. Oepen, and H. Ibach, Phys. Rev. Lett. **75**, 2035 (1995).

[3] R. Allenspach, M. Stampanoni, and A. Bischof, Phys. Rev. Lett. **65**, 3344 (1990).

[4] Z. Málek and V. Kamberský, Czech. J. Phys., Sect. B **8**, 416 (1958).

[5] C. Kooy and U. Enz, Philips Res. Rep. **15**, 7 (1960).

[6] R. Bodenberger and A. Hubert, Phys. Status Solidi A **44**, K7 (1977).

[7] *Ultrathin Magnetic Structures I*, edited by J. A. C. Bland and B. Heinrich (Springer, Berlin, 1994).

[8] J. Pommier, P. Meyer, G. Pénissard, J. Ferré, P. Bruno, and D. Renard, Phys. Rev. Lett. **65**, 2054 (1990).

[9] U. Gradmann, in *Handbook of Magnetic Materials*, edited by K. H. J. Buschow (Elsevier, Amsterdam, 1993), Vol. 7, p. 1.

[10] A. S. Arrott, J. Appl. Phys. **69**, 5212 (1991).
[11] A. Aharoni, *Introduction to the Theory of Ferromagnetism* (Oxford University Press, Oxford, 1996).
[12] An alternative explanation is that the energy stored outside the film vanishes in the absence of external magnetic fields because $\nabla \cdot \mathbf{B} = 0$ at the film surface leads to $\mathbf{H} = 0$ in free space.
[13] J. Shen, R. Skomski, M. Klaua, H. Jenniches, S. S. Manoharan, and J. Kirschner, J. Appl. Phys. **81**, 3901 (1997).
[14] A. Aharoni, Rev. Mod. Phys. **34**, 227 (1962).
[15] W. F. Brown, *Micromagnetics* (Wiley, New York, 1963).
[16] A. Aharoni, Phys. Status Solidi **16**, 3 (1966).
[17] Y. Yafet and E. M. Gyorgy, Phys. Rev. B **38**, 9145 (1988).
[18] H.-P. Oepen, M. Speckmann, Y. Millev, and J. Kirschner, Phys. Rev. B **55**, 2752 (1997).
[19] B. Kaplan and G. A. Gehring, J. Magn. Magn. Mater. **128**, 111 (1993).
[20] Y. Millev, J. Phys.: Condens. Matter **8**, 3671 (1996).
[21] I. Booth, A. B. MacIsaac, J. P. Whitehead, and K. De'Bell, Phys. Rev. Lett. **75**, 950 (1995).
[22] R. Skomski and N. M. Dempsey, in *Interstitial Intermetallic Alloys*, edited by F. Grandjean *et al.*, NATO Proceedings (Kluwer, Dordrecht, 1995), p. 653.
[23] J. A. Osborn, Phys. Rev. **67**, 351 (1945).
[24] R. Skomski and J. M. D. Coey, Phys. Rev. B **48**, 15 812 (1993).
[25] P. W. Anderson, Phys. Rev. **109**, 1492 (1958).
[26] R. Skomski, J. Giergiel, and J. Kirschner, IEEE Trans. Magn. **32**, 4576 (1996).
[27] C. Kittel, Rev. Mod. Phys. **21**, 541 (1949).
[28] For comparable domain configurations in cylinders, see Ref. 11.
[29] The x and x' integrations extend from $-\infty$ to $+\infty$ and imply $s(x) = 0$ outside the film.